PROCEEDINGS, 50th Workshop on Geothermal Reservoir Engineering
Stanford University, Stanford, California, February 10-12, 2025
SGP-TR-229

Comparative Study of Enhanced Geothermal System Supply Curves Across CONUS From Two Temperature Models Using the Renewable Energy Potential (reV) Model

Karthik Menon, Whitney Trainor-Guitton, Sophie-Min Thomson, Pavlo Pinchuk, Nicole Taverna, Reid Olson, and Galen Maclaurin

National Renewable Energy Lab (NREL), Golden, CO 80401

Karthik.Menon@nrel.gov

Keywords: EGS, reV, Stanford temperature model, Southern Methodist University temperature model, supply curves, LCOE

ABSTRACT

Enhanced geothermal systems (EGS) have had recent breakthroughs within the geothermal sector. These breakthroughs are reflected in the National Renewable Energy Laboratory (NREL) 2024 Annual Technology Baseline and will result in updated EGS supply curves (i.e., the available resource capacity relative to cost). Our research uses NREL's Renewable Energy Potential (reV) model to compare EGS supply curves across the conterminous United States (CONUS) for two different temperature models: the Stanford temperature model (STM) and the Southern Methodist University temperature model (SMU). The reV model provides the levelized cost of energy (LCOE) at a consistent resolution across CONUS, taking into consideration transmission costs and constraints as well as technical exclusions pertaining to sensitive cultural, ecological, or infrastructure locations. In addition to a countrywide analysis of both models, we also conducted a regional analysis of Texas. We observed the STM had, on average, lower temperatures across different depths, resulting in slightly higher mean and median LCOEs as compared to the SMU temperature model at the same depths. In the regional analysis for Texas, however, when we compared only the common points between the two temperature models, the STM had lower median and mean LCOEs compared to SMU due to higher temperatures at depths greater than 5 km.

1. INTRODUCTION

Advances in geothermal technologies have expanded the potential for geothermal development. Enhanced geothermal systems (EGS) are expected to play an important role in this expansion. Recent results from Fervo's Project Red site (Norbeck et al. 2024), in which they were able to successfully produce power and showcase the potential for cost reductions through previous outcomes, have increased interest in developing EGS resources.

A solid understanding of supply curves at a regional level provides greater insight into geothermal resource potential within the conterminous United States (CONUS). Recently, (Pinchuk et al., 2023) developed a geothermal module within the Renewable Energy Potential (reV) model to produce CONUS EGS supply curves, using the latest the National Renewable Energy Laboratory (NREL) 2024 Annual Technology Baseline (ATB) cost projections consistent with Fervo's progress and excluding certain regions such as defense land, interstate highways, buildings, and other lands not available for geothermal development.

In this paper, we compare the EGS supply curves across CONUS obtained from the reV model using two temperature models as input—the Stanford temperature model (STM) (Aljubran and Horne 2024b) and the Southern Methodist University temperature model (SMU; Blackwell et al. 2011). We further demonstrate how the models vary at depths in different geographic regions and how they result in differing Levelized Cost of Energy (LCOE) values. In addition, we compare LCOE with two different cost assumptions (2030 and 2035 costs) from the ATB (Mirletz et al. 2024). Furthermore, we discuss a regional scale analysis of EGS supply curves across Texas and the correlation between the supply curves and known geothermal resources.

2. METHODOLOGY

In this section, we present the workflow used in estimating the supply curves for both temperature models. We emphasize capacity estimates, particularly how they differ across both models. A regional analysis of Texas is included to showcase the performance of each model for observed sites found in the literature.

2.1 Geothermal Electricity Technology Evaluation Model Defaults

The Geothermal Electricity Technology Evaluation Model (GETEM) was developed for financial and performance calculations for geothermal power projects (Entingh et al. 2006). GETEM default values were used in reV to generate supply curves. These include capital and operating costs as determined by the advanced scenario in the ATB[1] for predictions of 2035 (Lopez et al. 2025) and default performance assumptions such as Production Well Flow Rate (110 kg/s per well), Plant Efficiency (80%), and Ratio of Injection Wells

[1] For complete assumptions in the ATB see https://atb.nrel.gov/electricity/2024/geothermal

to Production Wells (0.75). These are important to keep in mind because they determine the capacities produced on large spatial extents via reV. As noted in Chen et al. (2024), the flow value was set to 120 kg/s for the EGS Earthshot Analysis (Augustine et al. 2023), and Fervo reported values between 63 kg/s and 78 kg/s in their recent white paper (Norbeck et al. 2024).

2.2 CONUS Enhanced Geothermal Systems Estimates

A single method for estimating power density from temperature was used: an exponential relationship (Wilmarth et al. 2021). The exponential method was developed from regressing reservoir temperature and nameplate capacity for 103 operating geothermal fields across the world (Wilmarth et al. 2021):

$$\frac{MegaWatt}{km^2} = 0.408 \cdot e^{0.014 \cdot Reservoir\ Temperature}$$

We used both models (STM and SMU) and the exponential method to generate capacity (megawatt electric) estimates, which were input into reV. The supply curves were generated through NREL's reV workflow with the steps listed in Figure 1. Each of the steps in the workflow is discussed in detail in the succeeding subsections.

Once these supply curves were generated, we used the following metrics for comparison (only for the exponential method):

- Average and total capacity (in gigawatts, GW)
- Median site LCOE as well as LCOE all in (including transmission costs)
- Temperature and site LCOE values within Texas.

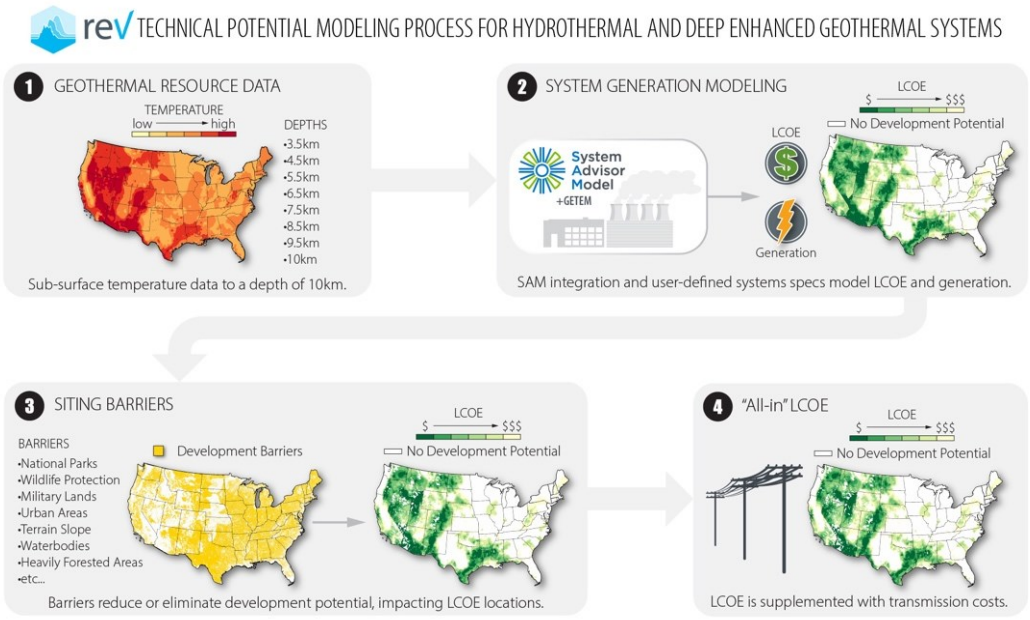

Figure 1: reV workflow for supply curve generation. (Graphic by NREL)

2.2.1 Geothermal Resource Data

The main input variable that results in varying LCOEs is the temperature. As mentioned in Section 2.2, the exponential model is used to generate capacity from temperature. The resource dataset is then input into the reV workflow to generate supply curves. SMU contains temperatures from 3.5 km to 10 km, whereas STM has temperatures from 1 to 7 km. The resource data in this study were limited to depths ranging from 1 to 7 km in intervals of 1 km each, and interpolation (in-built reV function) was used on the SMU model to obtain temperatures at the same depth as the STM. The resolution for STM temperature plots is 18 km^2, whereas the resolution NREL uses for SMU temperature plots is 6.25 km^2 (original SMU resolution is around 64 km^2). reV uses a temperature threshold for EGS projects and considers points having temperatures greater than or equal to 120°C and less than or equal to 375°C, as temperatures above this limit are characterized as "supercritical" temperatures when water is used as the reservoir fluid, whereas temperatures below 120°C are deemed too low for power production. The area represented by a point varies based on the model due to different spatial resolutions.

By visualizing the temperature distributions across CONUS for each model, one can identify regions with possibly low LCOE values. We observed the 75th percentile for temperatures was higher for the SMU model than for the Stanford model (Figure 2 and Figure 3). In Figure 2 and Figure 3, only temperatures above the 75th percentile of SMU temperatures at a given depth (in this case, 2,000 and 5,000 m, respectively) are displayed. Locations where higher temperatures are observed in one model but not the other gave us an indication of where LCOEs would differ significantly. For instance, in Figure 3, the STM temperatures in Western California are a lot higher than the SMU temperatures, which should result in a lower LCOE for that region. A similar observation can be seen in the Trans-Pecos region of West Texas in the SMU model in Figure 2 and Figure 3 and is discussed in more detail in the Texas regional analysis.

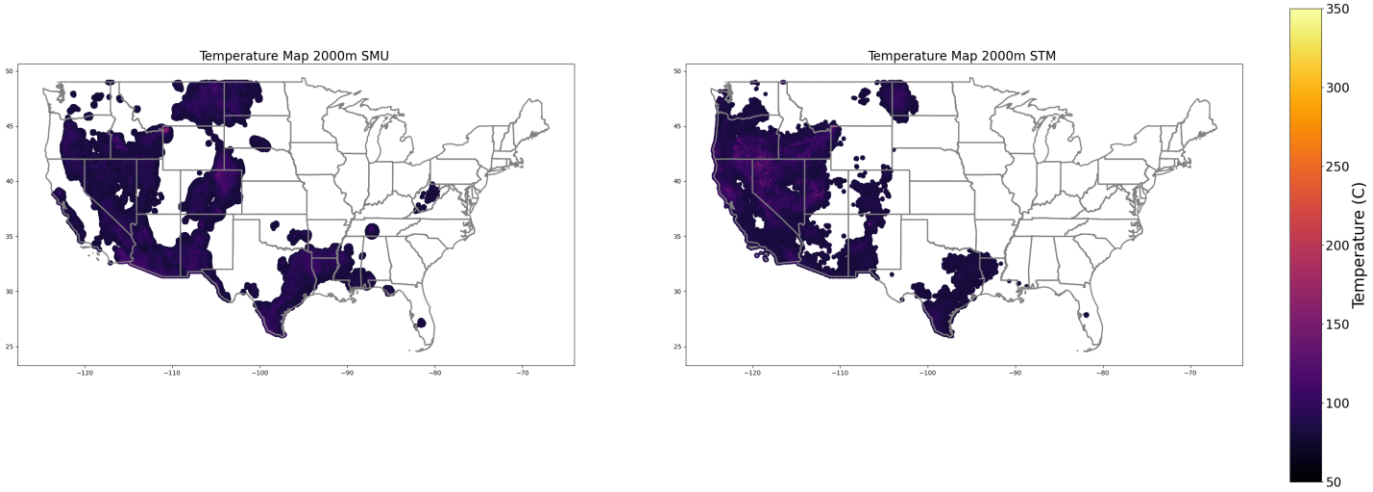

Figure 2: Temperature plots for points with temperatures greater than p75 (75°C) of SMU at 2,000 m.

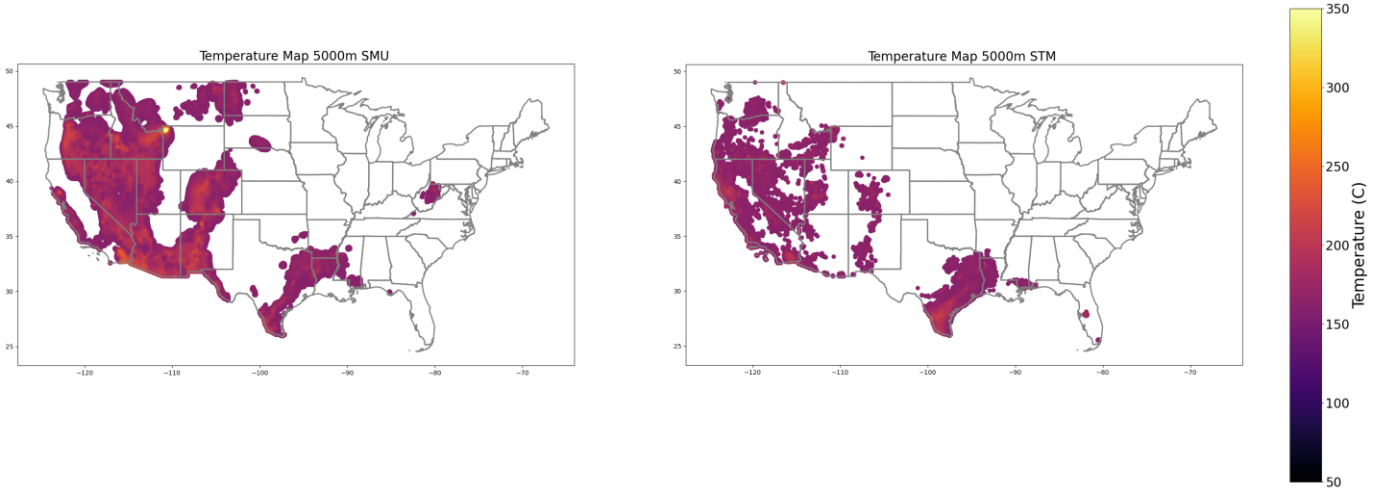

Figure 3: Temperature plots for points with temperatures greater than p75 (140°C) of SMU at 5,000 m.

2.2.2 Levelized Cost of Energy Generation Using the System Advisor Model

The system generation step in the workflow uses the System Advisor Model (SAM) to generate hourly generation profiles and LCOE based on user-defined plant configurations (Lopez et al. 2025) and GETEM default values described in section 2.1 Geothermal Electricity Technology Evaluation Model Defaults. The capital costs, operating costs, and other financing assumptions are obtained using the 2035 costs from the 2024 Annual Technology Baseline (ATB) (Mirletz et al. 2024). LCOE is calculated using the following formula:

$$LCOE = \frac{(FIXED\ CHARGE\ RATE \cdot CAPEX + FIXED\ OPERATION\ AND\ MAINTENANCE\ COSTS)}{CAPACITY\ FACTOR \cdot \left(8760\ \frac{hours}{year}\right)}$$

The ATB uses three scenarios for technology innovation that reduce the costs for future years—conservative (today's technology with little innovation), moderate (today's technology with widespread adoption), and advanced (new technology architectures and innovations) (Mirletz et al. 2024). In this work, we used the advanced scenario, inspired by the results of the recent Fervo case study (Norbeck et al. 2024). For EGS, the advanced scenario uses a learning rate of 35% from 2022 to 2035, followed by a 0.5% decline after that (Mirletz et al. 2024). The various ATB parameters for the advanced scenario are listed in Table 1, and the drilling costs (2035 costs calculated using the GeoVision ideal drilling cost curve (Lowry et al., 2017)) per well for each depth are listed in Figure 4. More information regarding these characteristics can be found in the reV annual report (Lopez et al. 2025).

Table 1: ATB advanced scenario geothermal technology characteristics from 2035 (Lopez et al. 2025).

Plant Characteristic	ATB Values
Fixed charge rate (%)	6.348
Capital expenditure ($/kW)	4,307
Fixed operational expenditure ($/kW)	119
Plant conversion type	Binary
Plant efficiency (%)	80
Change in pressure across the reservoir (psi-h/1,000 lb)	0.4
Wet bulb temperature (°C)	15
Ambient pressure (psi)	14.7
Production well flow rate (kg/s)	110
Pump efficiency (%)	67.5
Pressure difference across surface equipment (psi)	40
Excess pressure at pump suction (psi)	50
Production well diameter (inches)	12.25
Production pump casing size (inches)	9.625
Injection well diameter (inches)	12.25
Injection pump casing size (inches)	11.5
Number of confirmation wells	0
Ratio of injection wells to production wells	0.75
Well type	Vertical Open-Hole

kg = kilogram; kW = kilowatt; lb = pound; psi = pounds per square inch; psi-h = pounds per square inch-hour; s = second.

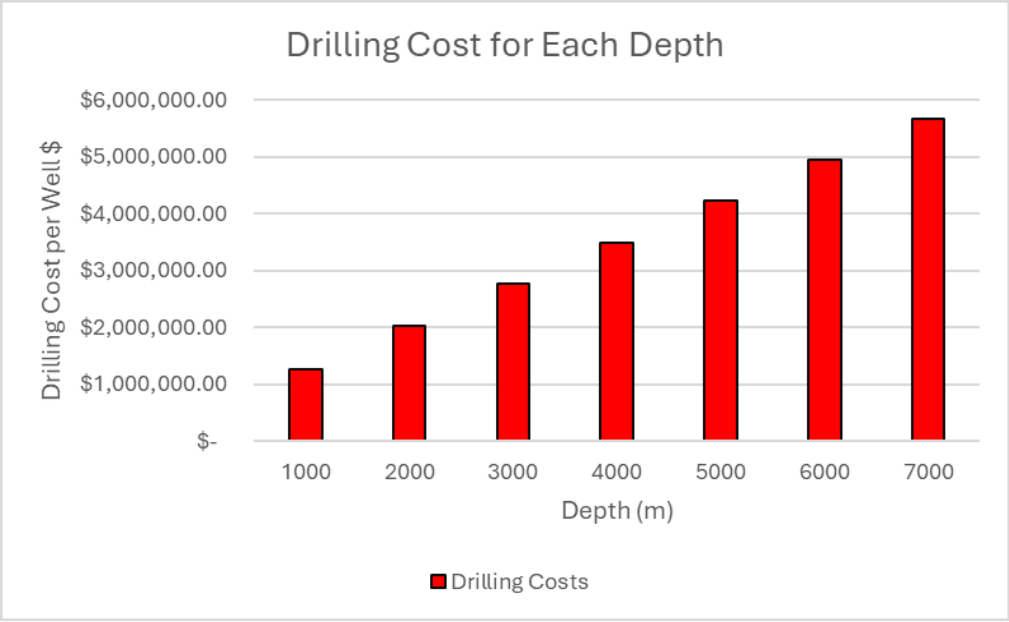

Figure 4: Drilling costs per well for each depth slice (based on 2035 costs).

The LCOE obtained from this step is the "LCOE site" value. This value denotes the LCOE for geothermal electricity production on site, without including any transmission costs.

2.2.3 Technical Exclusions for Geothermal Development

Technical exclusions for geothermal development were applied using a collection of layers that aggregate cultural, environmental, infrastructural, or regulatory considerations across CONUS. For the sake of brevity, only a few of the exclusions used are listed in Table 2, whereas the entire set can be found in the reV 2025 annual report (Lopez et al. 2025). In general, the assumptions for geothermal exclusions follow those for utility photovoltaics, except for the following:

- No property line setbacks were applied for geothermal projects.
- Solar moratoriums were not applied to geothermal development (there are no explicit geothermal bans).
- Exclusions based on terrain slope used a 25% value for geothermal, which is the same as for wind but differs from the 5% used for utility-scale photovoltaics.
- No contiguous area filter was applied for geothermal given separation between geothermal power plants and wellfields.
- Habitats of greater prairie-chicken, Dixie Valley toad, and Tiehm's buckwheat (<2 km^2 for CONUS) were excluded from development.

Table 2: Technical exclusions for geothermal project development.

Category	Dataset
Defense	Ballistic missile silo setback, airport and runways, U.S. Department of Defense clear and accident potential zones.
Environmental	Bat hibernacula setbacks, karst depressions, U.S. Forest Service active grazing and Bureau of Land Management mature and old growth forests, National Land cover dataset—water and woody wetlands, desert tortoise, threatened and endangered species' core habitat, U.S. Fish and Wildlife Service, nationally significant agricultural lands.
Infrastructure	Designated transmission corridors, oil and gas well footprints, railroads and roads, geothermal plant locations.
Regulatory	Oil and gas pipelines, rail and road setbacks, transmission setback, water setback.
Terrain	Slope exclusion, mountainous landforms.

These technical exclusions were applied to generation profiles from the previous step, followed by adding transmission costs to generate the final supply curve with a spatial resolution of 11.5 km^2. The updated supply curve contains all the features produced during the previous step (with the exclusions) and an additional feature "LCOE All-in" (seen in Figure 1) that includes transmission costs (Lopez et al. 2025).

3. RESULTS

The results for LCOEs ("site" and "all-in") are compared in the following sections. A granular regional analysis of supply curves for Texas with corresponding temperature plots is also presented.

3.1 Enhanced Geothermal Systems CONUS-Wide Analysis

A comparison of average and total capacity (MW) for both temperature models is presented in Table 3, and the LCOE for supply curves using the latest ATB costs (2035) is provided in Table 4. The supply curves for SMU and STM can be seen in Figure 5. Due to the reV temperature threshold mentioned in section 2.2.1 (120°C–375°C), there are fewer points for shallower depths. When moving to deeper depths, the LCOE values tend to remain similar to those observed in shallower depths, however, the total capacity available increases for a fixed LCOE cutoff. For Instance, in Figure 5 for STM at a depth of 5000m and LCOE cutoff of $70/MWh there is roughly 2000 GW of capacity available, but when we reach a depth of 6000m, this capacity estimate doubles to around 4000 GW.

Table 3: Comparison between SMU and STM capacities.

Depth (m)	Number of Points		Median Capacity (MW)		Total Capacity (GW)	
	SMU	STM	SMU	STM	SMU	STM
1,000	12	26	45	15	0.9	0.5
2,000	62	682	44	14	4	20
3,000	7,210	5,358	67	39	668	364
4,000	19,979	16,814	111	85	2,693	1,803
5,000	29,912	29,300	135	107	5,190	3,910
6,000	45,356	49,506	137	104	8,803	7,046
7,000	53,828	55,658	146	133	9,197	9,296

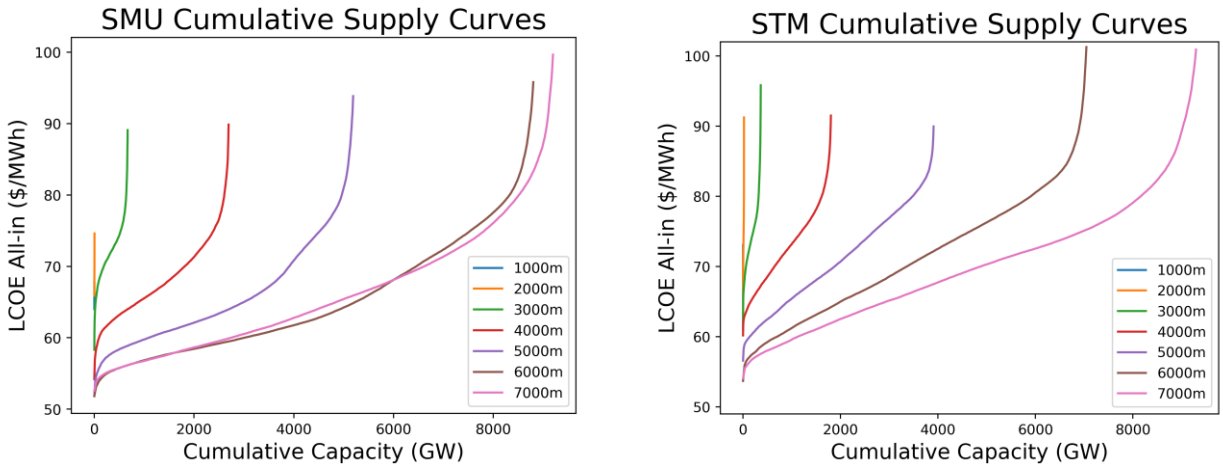

Figure 5: Cumulative Supply Curves for SMU (Left) and STM (Right)

Table 4: Median LCOE site and LCOE all-in for SMU and STM.

Depth	Median LCOE Site		Median LCOE All-In	
	SMU	**STM**	**SMU**	**STM**
1,000	$64	$63	$66	$68
2,000	$67	$68	$69	$75
3,000	$68	$69	$73	$76
4,000	$62	$68	$69	$75

5,000	$59	$67	$67	$74
6,000	$62	$70	$69	$75
7,000	$63	$67	$68	$72

Box plots for LCOE site and all-in values are also given in Figure 6 and Figure 7. Although drilling costs increase as we progress deeper, the increase in temperatures and thereby capacity compensate for this increase and thus result in similar LCOE's across most depths. On average, there seem to be lower LCOE values for SMU than STM across most depths. The blue box represents the three quartiles of the distribution (p25, p50, and p75). The whiskers on the plot denote points that fall within 1.5 IQRs (Inter quartile ranges) of the upper and lower quartile. LCOE site values (Figure 6) do not seem to have many outliers, except for certain instances at depths of 2,000 and 3,000 m. The LCOE all in box plots (Figure 7) paint a different picture, as there appear to be several outliers across multiple depths. This could be related to areas with geothermal potential but poor transmission infrastructure, such as certain parts of West Virginia and Western Pennsylvania with high levelized costs of transmission.

For depths greater than 2,000 m, median LCOE is the lowest at 5,000 m for SMU, although it is the lowest at 7,000 m for STM. The median LCOEs for deeper depths are higher than the results observed in Aljubran and Horne (2024a), and the total capacity (22,438 GW) for depths 1-7km for STM is smaller when compared to 35,808 GW in (Aljubran & Horne, 2024c)), potentially due to the use of the exponential method (mentioned in section 2.2) for resource potential estimation as compared to the FGEM (Flexible Geothermal Economics Modeling) tool used in (Aljubran and Horne (2024a); (Aljubran & Horne, 2024c)) and (Aljubran & Horne, 2025).

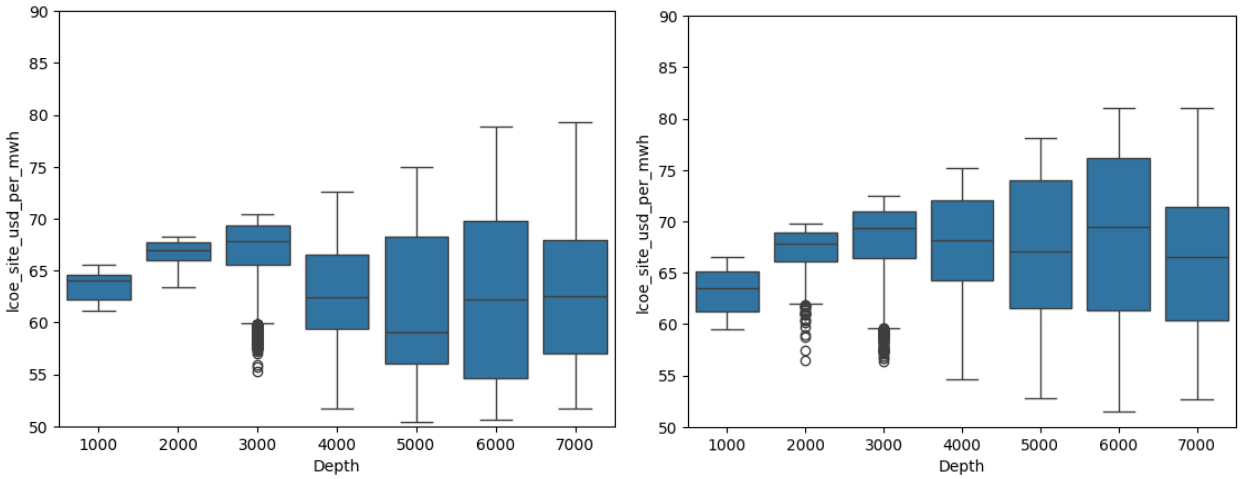

Figure 6: SMU (Left) vs STM (Right) LCOE site box plot for all depths.

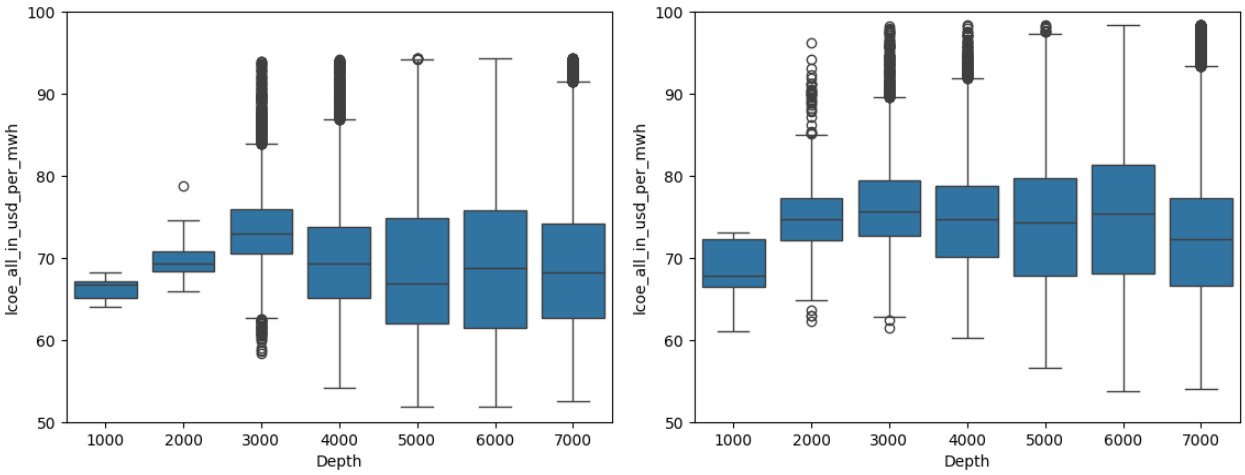

Figure 7: SMU (left) vs STM (right) LCOE all-in box plot for all depths.

The spatial distribution of site LCOE for depths of 5,000 m and 6,000 m is shown in Figure 8 and Figure 9. An interesting observation is the available area for EGS at 6,000 m increases suddenly for both STM and SMU, which is validated by looking at the number of points in Table 3Table 3: Comparison between SMU and STM capacities. On average, SMU LCOE values are much lower in the western United States, whereas STM values are lower in areas such as western and northwestern California, the Gulf Coast, and parts of Florida. When depth changes from 5,000 m to 6,000 m, several new EGS opportunities arise, particularly in the Midwest and parts of the East Coast. This conclusion is also supported by the supply curves in Figure 5.

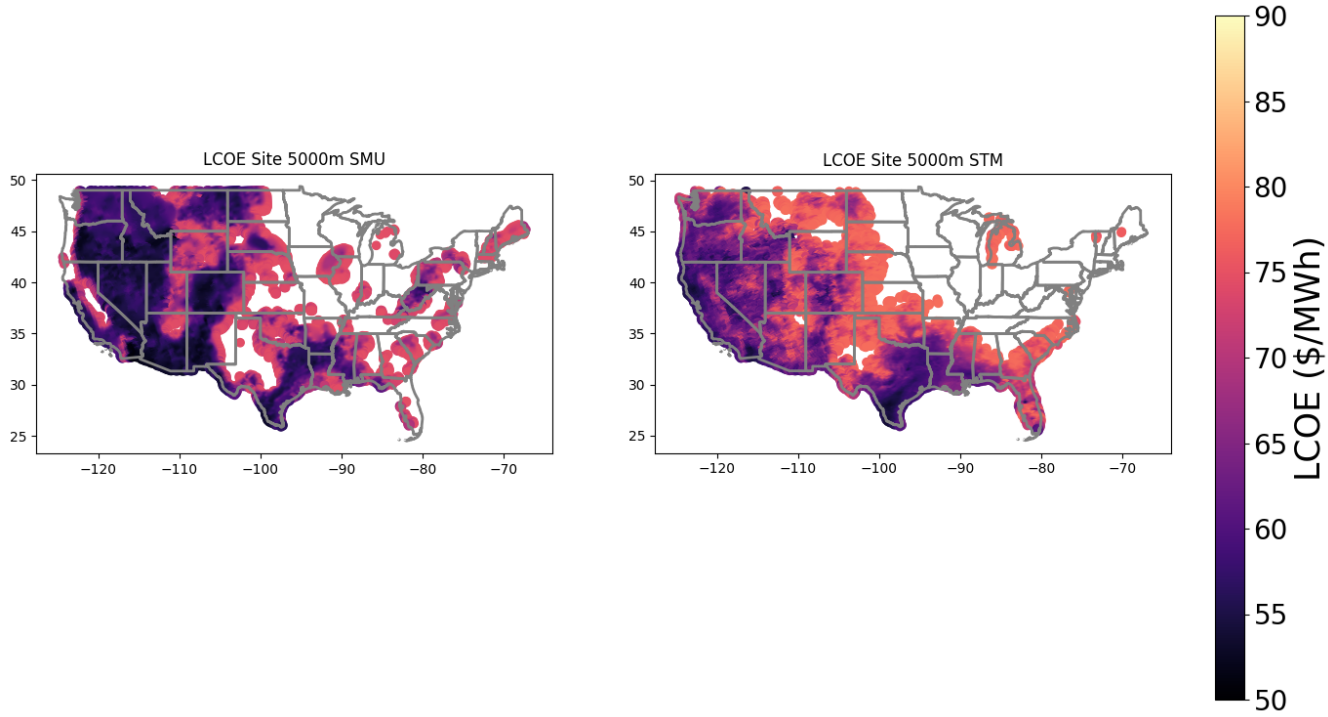

Figure 8: LCOE "site" values at 5,000 m.

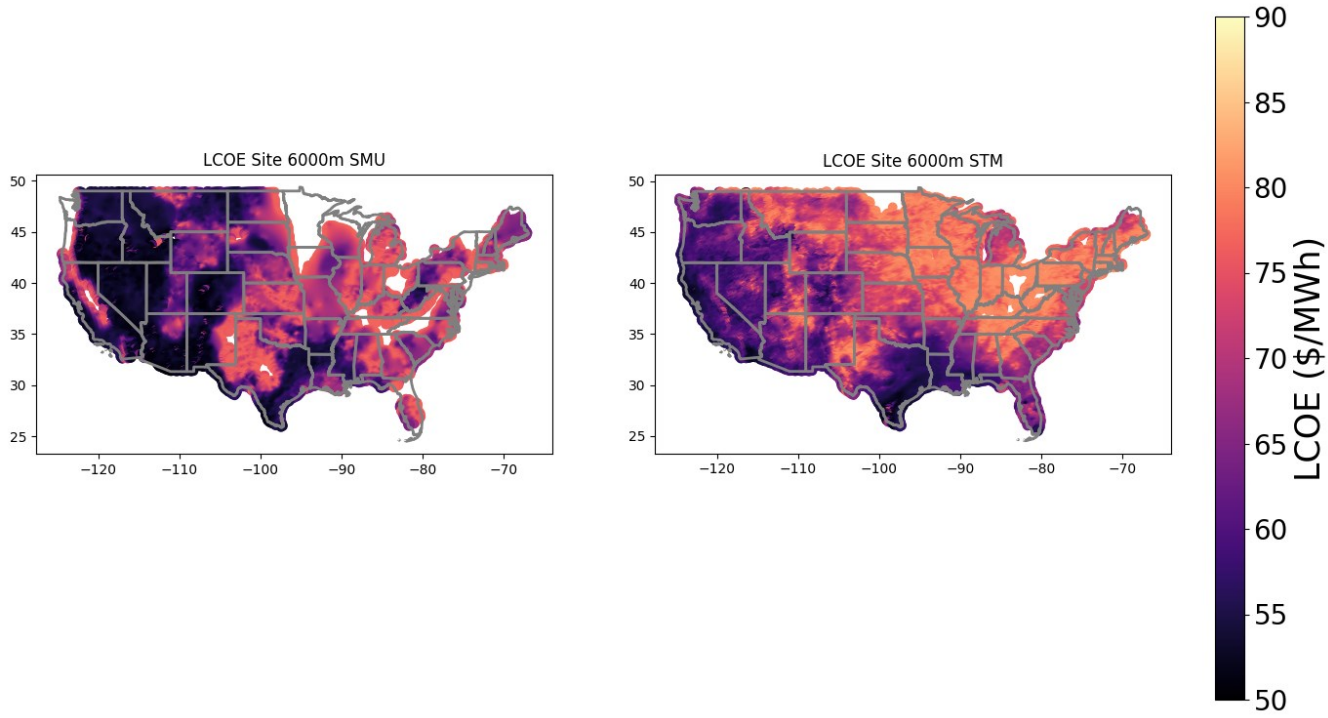

Figure 9: LCOE "site" values at 6,000 m.

3.1.1 LCOE Comparison—2030 versus 2035 ATB Costs

As geothermal operators continue to learn more about individual projects, project costs decrease over the years. This is reflected in the ATB cost reports. To quantify this reduction in geothermal supply curves, we compared the resultant LCOEs (including transmission costs) when using the 2030 costs versus 2035 costs for the advanced scenario in the ATB. The comparison for LCOE for both STM and SMU using the updated costs is given in Figure 10. On average, the LCOE of SMU supply curves decreased $18/MWh (megawatt-hour), whereas the STM-based curves decreased by $19/MWh.

Table 5: LCOE all-in for ATB 2030 versus 2035.

Depth(m)	SMU		STM	
	2030 Median LCOE All-In	2035 Median LCOE All-In	2030 Median LCOE All-In	2035 Median LCOE All-In
1,000	$84	$66	$87	$68
2,000	$85	$69	$94	$75
3,000	$92	$73	$95	$76
4,000	$87	$69	$94	$75
5,000	$84	$67	$92	$74
6,000	$86	$69	$94	$75
7,000	$86	$68	$90	$72

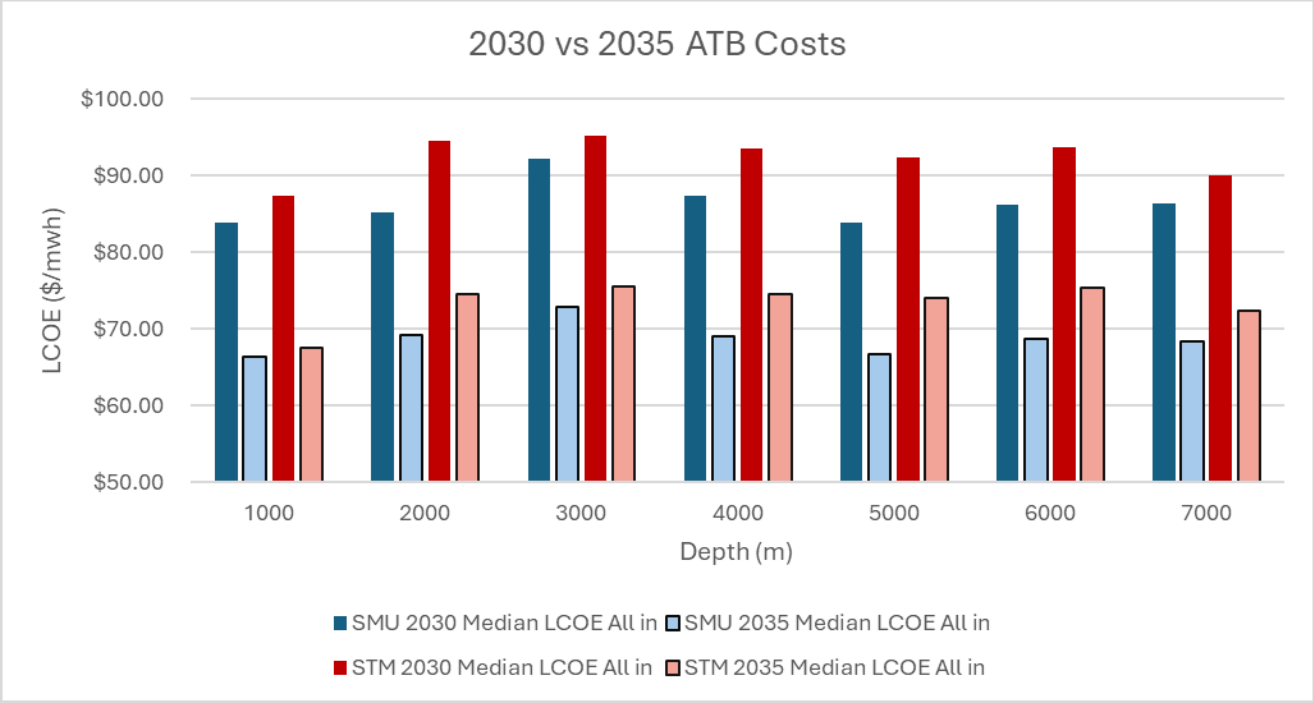

Figure 10: Comparison of LCOE using 2035 (lighter shades) versus 2030 costs for SMU and STM.

3.2 Enhanced Geothermal Systems Texas Analysis

Figure 11 highlights various probable and known geothermal resources in Texas. There are four major regions with possible geothermal potential: the Trans-Pecos and Delaware Basin that form part of the Basin and Range Province of West Texas, the Anadarko Basin, the Maverick Basin in south-central Texas, and the geopressured Gulf Coast zone. Of the two temperature models, SMU shows a greater tendency to replicate these locations (particularly in West Texas, as seen in the temperature plots), whereas both SMU and STM showcase geothermal potential within the Gulf geopressured zone. One important fact to remember is in the SMU maps, due to lower spatial resolution, high temperatures may extend to regions where there may not be significant geothermal potential—that is, these maps may overestimate the spatial extent of potential geothermal sites.

Although the depths for known geothermal resources in West Texas (Trans-Pecos region), according to Figure 11**,** are shallow, the geothermal gradients and heat flow in these regions are quite high, based on a recent study conducted by the Bureau of Economic Geology at UT Austin (Wisian et al. 2024). Furthermore, the "benchmark" depths for temperatures of 150°C, 200°C, and 250°C within the border region are 2,600 m, 3,700 m, and 4,770 m, respectively (Wisian et al. 2024). This trend can be visualized by the temperature at depth plots for SMU in Figure 12. Despite its good correlation with the Presidio County study, unless more exploration campaigns and tests are run in regions neighboring Presidio County, we cannot conclude definitively whether the SMU model showcases geothermal potential in West Texas.

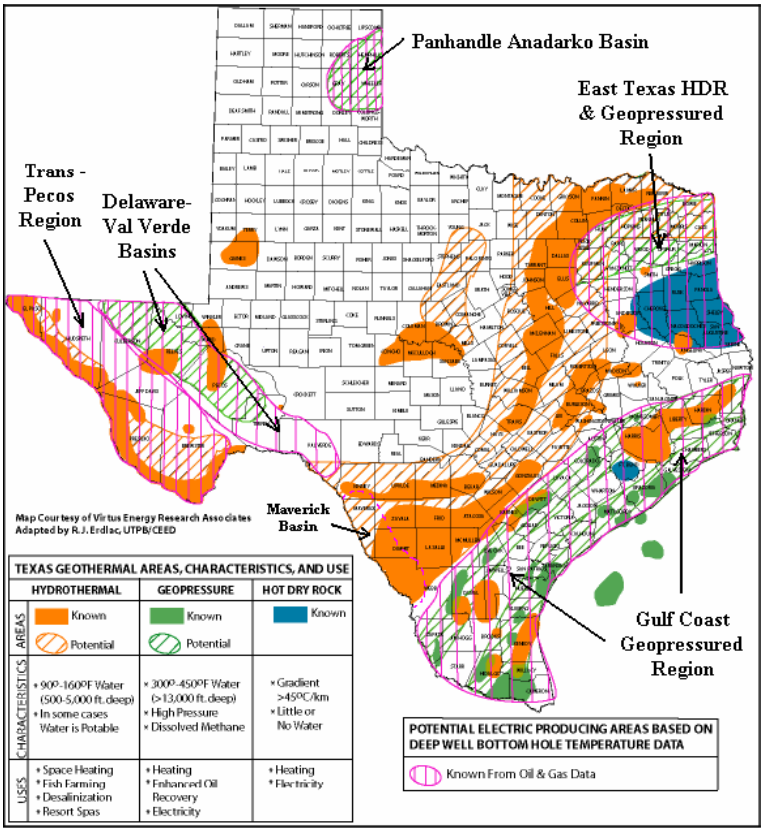

Figure 11: Known geothermal resources in Texas (Erdlac et al. 2007).

3.2.1 Texas LCOE Analysis

Figure 12 is a visual representation of median LCOE at depths deeper than 3,000 m with associated temperature plots for common points (both these supply curves have the same resolution of 11.5 km^2) between SMU and STM supply curves. For depths shallower than 3,000 m, due to the small number of points in the supply curves of both models, no common points were found; thus, these depths were not included. Although the CONUS-wide plots for LCOE are lower in SMU than in STM for shallower depths in Texas, STM has lower LCOE costs at deeper depths (<5,000 m), due to higher temperatures (Figure 12).

However, as mentioned in the previous section, SMU maps contain higher temperatures in West Texas, coinciding with possible geothermal regions. STM, on the other hand, has higher temperatures in South Texas and along the Gulf Coast across all depths when compared to SMU. This could be attributed to the fact that STM incorporated more geophysical datasets, such as magnetic anomaly and electrical conductivity. The LCOE median values are calculated by considering only common points between SMU and STM, obtained through an overlay operation.

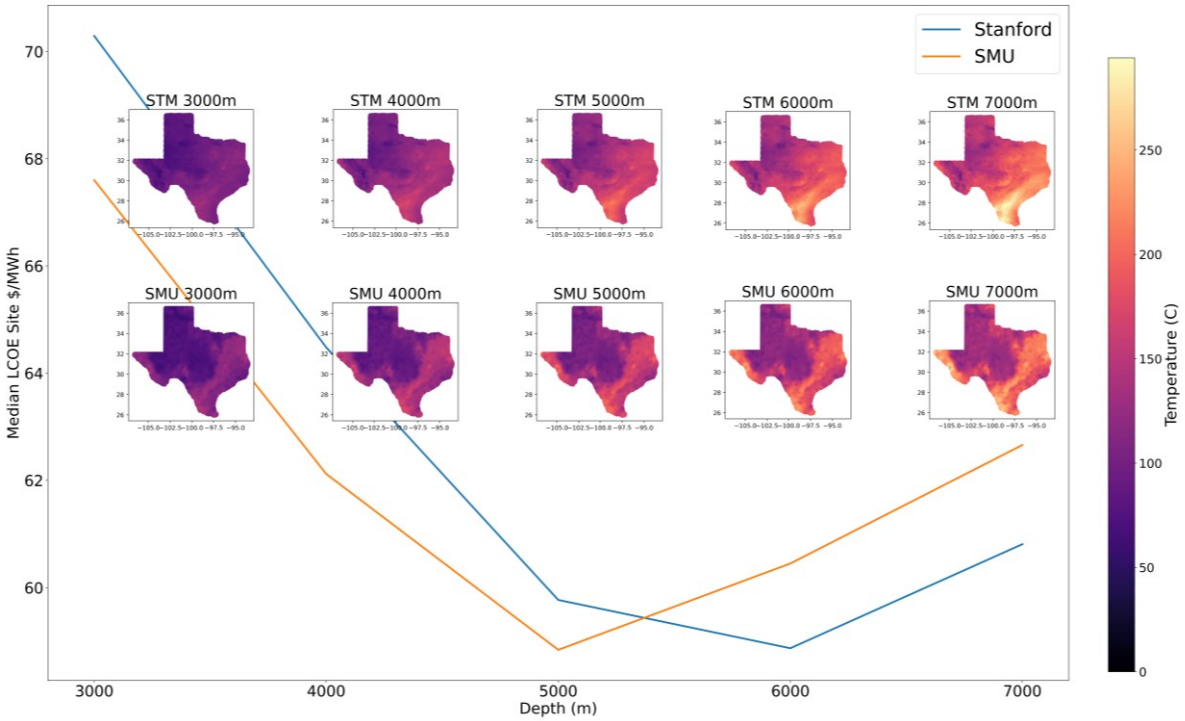

Figure 12: Median site LCOE ($/MWh) for SMU and STM with temperature at depth plots for Texas.

4. CONCLUSIONS

In this work, we used two available temperature models to generate EGS supply curves across the contiguous United States and compared them to each other. SMU supply curves had a lower median LCOE than STM due to higher temperatures at the same depth and had higher total capacities except for the deepest depth—7,000 m. The STM model had more possible sites at shallower depths compared to SMU and showcased greater geothermal potential in areas such as southern Florida, western California, and the Texas Gulf Coast when compared to the SMU model. Furthermore, moving from 2030 ATB to 2035 ATB costs, results in a large decrease in the supply curve LCOE and provide a good upper bound for operators working on projects within these regions.

To conclude, this work aims to highlight regions with high geothermal potential and showcase the sensitivity input costs can have on the supply curve. As more EGS projects are initiated, resulting in more data from actual projects, greater clarity will be obtained for LCOE.

Future work will look at incorporating uncertainty into the supply curve and possibly integrating the results with capacity expansion models such as NREL's Regional Energy Deployment System (ReEDS) model for power systems planning.

ACKNOWLEDGMENTS

This work was authored by the National Renewable Energy Laboratory, operated by Alliance for Sustainable Energy, LLC, for the U.S. Department of Energy (DOE) under Contract No. DE-AC36-08GO28308. Funding provided by U.S. Department of Energy Office of Energy Efficiency and Renewable Energy Geothermal Technologies Office. The views expressed in the article do not necessarily represent the views of the DOE or the U.S. Government. The U.S. Government retains and the publisher, by accepting the article for publication, acknowledges that the U.S. Government retains a nonexclusive, paid-up, irrevocable, worldwide license to publish or reproduce the published form of this work, or allow others to do so, for U.S. Government purposes. We thank Sean Porse and Andy Adams (U.S. Department of Energy Office of Energy Efficiency and Renewable Energy Geothermal Technologies Office) for their insight and support of the project.

REFERENCES

Aljubran, M., and Horne, R. (2024a). "Techno-economics of Enhanced Geothermal Systems Across the United States Using Novel Temperature-at-Depth Maps." Presented at 49th Workshop on Geothermal Reservoir Engineering Stanford University, Stanford, California, February 12–14, 2024. SGP-TR-227. https://pangea.stanford.edu/ERE/db/GeoConf/papers/SGW/2024/Aljubran.pdf.

Aljubran, M. J., and Horne, R. N. (2024b). "Thermal Earth Model for the Conterminous United States Using an Interpolative Physics-Informed Graph Neural Network." *Geothermal Energy* 12 (1): 25. https://doi.org/10.1186/s40517-024-00304-7.

Aljubran, M. J., & Horne, R. N. (2024c). Power supply characterization of baseload and flexible enhanced geothermal systems. Scientific Reports, 14(1), 17619. https://doi.org/10.1038/s41598-024-68580-8

Aljubran, M. J., & Horne, R. N. (2025). Techno-economics of geothermal power in the contiguous United States under baseload and flexible operations. Renewable and Sustainable Energy Reviews, 211, 115322. https://doi.org/10.1016/j.rser.2024.115322

Augustine, C., Fisher, S., Ho, J., Warren, I., and Witter, E. (2023). *Enhanced Geothermal Shot Analysis for the Geothermal Technologies Office*. Golden, CO: National Renewable Energy Laboratory. NREL/TP-5700-84822. https://www.osti.gov/servlets/purl/1922621/.

Blackwell, D., Richards, M., Frone, Z., Batir, J., Ruzo, A., Dingwall, R., and Williams, M. (2011). Temperature-At-Depth Maps For the Conterminous US and Geothermal Resource Estimates. Presented at Geothermal Resources Council 2011 Annual Meeting, San Diego, California, October 24, 2011–October 27, 2011. https://www.osti.gov/biblio/1137036.

Chen, C., Merino-Garcia, D., Lines, T. D. G. H., and Cohan, D. S. (2024). "Geothermal Power Generation Potential in the United States by 2050." *Environmental Research: Energy* 1 (2): 025003. https://doi.org/10.1088/2753-3751/ad3fbb.

Entingh, D. J., Pike, R., and Lane, S. (2006). *DOE Geothermal Electricity Technology Evaluation Model (GETEM): Volume I—* Technical Reference Manual. https://www1.eere.energy.gov/geothermal/pdfs/getem_vol_i_technical_manual.pdf

Erdlac, R. J., Armour, L., Lee, R., Snyder, S., Sorensen, M., Matteucci, M., and Horton, J. (2007). ONGOING RESOURCE ASSESSMENT OF GEOTHERMAL ENERGY FROM SEDIMENTARY BASINS IN TEXAS. PROCEEDINGS, Thirty-Second Workshop on Geothermal Reservoir Engineering Stanford University, Stanford, California, January 22-24, 2007 SGP-TR-183. https://earthsci.stanford.edu/ERE/pdf/IGAstandard/SGW/2007/erdlac.pdf

Lopez, A., Zuckerman, G. R., Pinchuk, P., Gleason, M., Rivers, M., Roberts, O., Williams, T., Heimiller, D., Thomson, S.-M., Mai, T., and Cole, W. (2025). *Renewable Energy Technical Potential and Supply Curves for the Contiguous United States: 2024 Edition*. Golden, CO: National Renewable Energy Laboratory. NREL/TP-6A20-91900. https://www.nrel.gov/docs/fy25osti/91900.pdf.

Lowry, T. S., Finger, J. T., Carrigan, C. R., Foris, A., Kennedy, M. B., Corbet, T. F., Doughty, C. A., Pye, S., and Sonnenthal, E. L. (2017). GeoVision Analysis Supporting Task Force Report: Reservoir Maintenance and Development. osti.gov/servlets/purl/1394062

Mirletz, B., Vimmerstedt, L., Stehly, T., Stright, D., Cohen, S., Cole, W., Duffy, P., et al. (2024). 2024 Annual Technology Baseline (ATB) Cost and Performance Data for Electricity Generation Technologies [Dataset]. National Renewable Energy Laboratory (NREL); Open Energy Data Initiative (OEDI). https://doi.org/10.25984/2377191.

Norbeck, J. H., Gradl, C., and Latimer, T. (2024). Deployment of Enhanced Geothermal System technology leads to rapid cost reductions and performance improvements. https://doi.org/10.31223/X5VH8C

Pinchuk, P., Thomsen, S.-M., Trainor-Guitton, W., Buster, G., & Maclaurin, G. (2023). Development of a Geothermal Module in reV: Quantifying the Geothermal Potential while Accounting for the Geospatial Intersection of the Grid Infrastructure and Land Use Characteristics. Geothermal Resources Council Transactions, 47, 2564–2586. https://www.geothermal-library.org/index.php?mode=pubs&action=view&record=1034921

Wilmarth, M., Stimac, J., and Ganefianto, G. (2021, October). Power Density in Geothermal Fields, 2020 Update. Proceedings World Geothermal Congress 2020+1, 1-8.

Wisian, K., Ross, M., Bhattacharya, S., Khaled, M., Young, B., Chapman, D., and Turan, A. (2024). Presidio County Geothermal Assessment. presidio_county_geothermal_assessment_final_v2.pdf